KJPP

Original Article ——————————————

MST1R as a potential new target antigen of chimeric antigen receptor T cells to treat solid tumors

Wen An[1], Ju-Seop Kang[1,*], Sukjoong Oh[2], and Ang Tu[3]

[1]Department of Pharmacology & Clinical Pharmacology Lab, [2]Department of Internal Medicine, College of Medicine, Hanyang University, Seoul 04763, Korea,
[3]Department of Pharmacy, Xiantao Hospital of Traditional Chinese Medicine, Xiantao 433000, China

*Correspondence
Ju-Seop Kang
E-mail: jskang@hanyang.ac.kr

ABSTRACT Although chimeric antigen receptor T cell (CAR-T) is a promising immunotherapy in hematological malignancies, there remain many obstacles to CAR-T cell therapy for solid tumors. Identifying appropriate tumor-associated antigens (TAAs) is especially critical for success. Using a bioinformatics approach, we identified common potential TAAs for CAR-T cell immunotherapy in solid tumors. We used the GEO database as a training dataset to find differentially expressed genes (DEGs) and verified candidates using the TCGA database, obtaining seven common DEGs (HM13, SDC1, MST1R, HMMR, MIF, CD24, and PDIA4). Then, we used MERAV to analyze the expression of six genes in normal tissues to determine the ideal target genes. Finally, we analyzed tumor microenvironment factors. The results of major microenvironment factor analyses showed that MDSCs, CXCL1, CXCL12, CXCL5, CCL2, CCL5, TGF-β, CTLA-4, and IFN-γ were significantly overexpressed in breast cancer. The expression of MST1R was positively correlated with TGF-β, CTLA-4, and IFN-γ. In lung adenocarcinoma, MDSCs, Tregs, CXCL12, CXCL5, CCL2, PD-L1, CTLA-4, and IFN-γ were significantly overexpressed in tumor tissues. The expression of MST1R was positively correlated with TGF-β, CTLA-4, and IFN-γ. In bladder cancer, CXCL12, CCL2, and CXCL5 were significantly overexpressed in tumor tissues. MST1R expression was positively correlated with TGF-β. Our results demonstrate that MST1R has the potential as a new target antigen for treating breast cancer, lung adenocarcinoma, and bladder cancer and may be used as a progression indicator for bladder cancer.

INTRODUCTION

Chimeric antigen receptor T cells (CAR-T) have attracted increasing attention for their unexpected potential in the treatment of hematological malignancies, including acute B-lymphocyte leukemia, B-cell non-Hodgkin's lymphoma, and multiple myeloma. CAR-T has become one of the most promising therapeutic methods in tumor immunotherapy. CAR-T cells are genetically engineered T cells that express non-MHC-restricted receptors to identify and eliminate cells that express specific target antigens. At present, for treatment of B-cell lymphoma, CD19 and BCMA antigens are available [1,2].

The premise of solid tumor CAR-T cell therapy is to find the ideal target antigen. Unlike cancers in which tumor cells usually express the B cell marker CD19, such as acute lymphoblastic leukemia (ALL) or chronic lymphoblastic leukemia, solid tumors seldom express tumor-specific antigens. For most solid tumors, it is more common to find tumor-associated antigens (TAAs), in which the antigen is enriched in tumors but is poorly expressed in normal tissues [3]. CAR-T TAA is expressed on the surfaces of all tumor cells but not on important organs or normal cell types (hematopoietic stem cells). Even low-level expression can cause serious side effects. Therefore, finding the ideal TAA has become the primary task of CAR-T cell therapy.

However, the TAA of most solid tumors is based on only one type of solid tumor, such as that of prostate cancer (PSCA, PSMA) or breast cancer (HER2, MUC1) [4,5]. Therefore, using bioinformatics technology, we sought to identify common potential TAAs for CAR-T cell immunotherapy in breast cancer, lung adenocarcinoma, and bladder cancer.

METHODS

Gene expression datasets

Training datasets (GSE21422, GSE65635, and GSE140797) were downloaded from the GEO database. The GSE21422 set contained 14 breast tumor tissue samples and five adjacent non-tumor samples. GSE65635 included eight samples of bladder tumor tissue and four samples of adjacent non-tumor. GSE140797 comprised seven lung tumor tissue samples and seven adjacent non-tumor samples. Validation datasets were downloaded from the Genomic Data Commons Data Portal (GDC Data Portal) (RRID:SCR_014514). We selected LUAD (lung adenocarcinoma), BRCA (breast cancer), and BLCA (bladder cancer) datasets with mRNA expression data and clinical features for correlation and survival analyses.

Screening of differentially expressed genes (DEGs)

We identified DEGs using the Linear Models for Microarray data (Limma) package in R [6]. The DEGs were identified using p-value < 0.05 and log2 (fold change) > 1. Meanwhile, volcano plots of the DEGs were visualized using the R gplots program. Common DEGs of GSE21422, GSE65635, and GSE140797 were identified by Venn diagram (https://bioinformatics.psb.ugent.be/webtools/Venn/). All common DEGs in these datasets were selected for further study.

Functional enrichment analysis

The Database for Annotation, Visualization, and Integrated Discovery (DAVID) bioinformatics resource consists of an integrated biological knowledge base and analytic tools aimed at systematically extracting biological meaning from large gene or protein lists [7,8]. In our study, DAVID was used to analyze the identified target genes according to the Kyoto Encyclopedia of Genes and Genomes (KEGG) and Gene Ontology (GO). KEGG is a knowledge base for systematic analysis of gene functions, while GO analysis predicts the functions of target genes from biological processes (BP), cell composition, and molecular function (MF). Functional annotation with p-value < 0.05 and enrichment score > 2.0 was considered statistically significant. The enrichment results were visualized by R.

Gene expression in normal tissues

MERAV is a powerful genome-wide analysis tool that can search multiple genes in parallel and compare gene expression between tissue types and between normal cells and cancer cells [9].

Immune infiltrate levels, expression analysis, and survival analysis

The marker genes of 28 types of immune cell in ssGSEA were obtained from a previous study [10]. Infiltration levels of different immune cell types were quantified by ssGSEA implementation R package gsva. Heatmaps of immune infiltration levels were generated using the R heatmap package. A visual scatterplot of Spearman correlations between MST1R expression of BRCA, LUAD, and BLCA and tumor infiltrating immune cells was generated using the ggplot2 function in R. We used the corrplot function of the corrplot R package to generate correlation diagrams of all variables. Survival analysis was conducted using the survival package in R.

Statistical analysis

Most of the statistical analyses were performed using the bioinformatic tools mentioned above. R software (version 4.2.0) was used for all remaining statistical analyses. Spearman correlation coefficients were calculated to evaluate correlations. p-values < 0.05 were considered statistically significant.

RESULTS

Identification of DEGs in GEO

In this study, after screening the GEO datasets of three cancers, the mRNA microarray datasets GSE21422, GSE65635, and GSE140797 with the best data quality were selected for analysis to obtain DEGs of respective breast cancer, bladder cancer, and lung adenocarcinoma tissues and of adjacent normal tissues for each. As shown in volcano plots (Fig. 1A–C), genes with p-value < 0.05 and logFC > 1 or <–1 were considered significant DEGs. In this study, only upregulated genes were considered. In GSE21422, 1,344 upregulated genes were screened. In GSE65635, a total of 1,195 upregulated genes were screened. In GSE140797, 1,594 upregulated genes were screened. Venn diagrams were used to identify 125 co-upregulated genes in the three datasets (Fig. 1D).

GO and KEGG enrichment analysis

To explore the biological functions of common DEGs, DAVID was used for enrichment analysis of GO and KEGG pathways. We found that DEGs, which are common in BP, were mainly involved
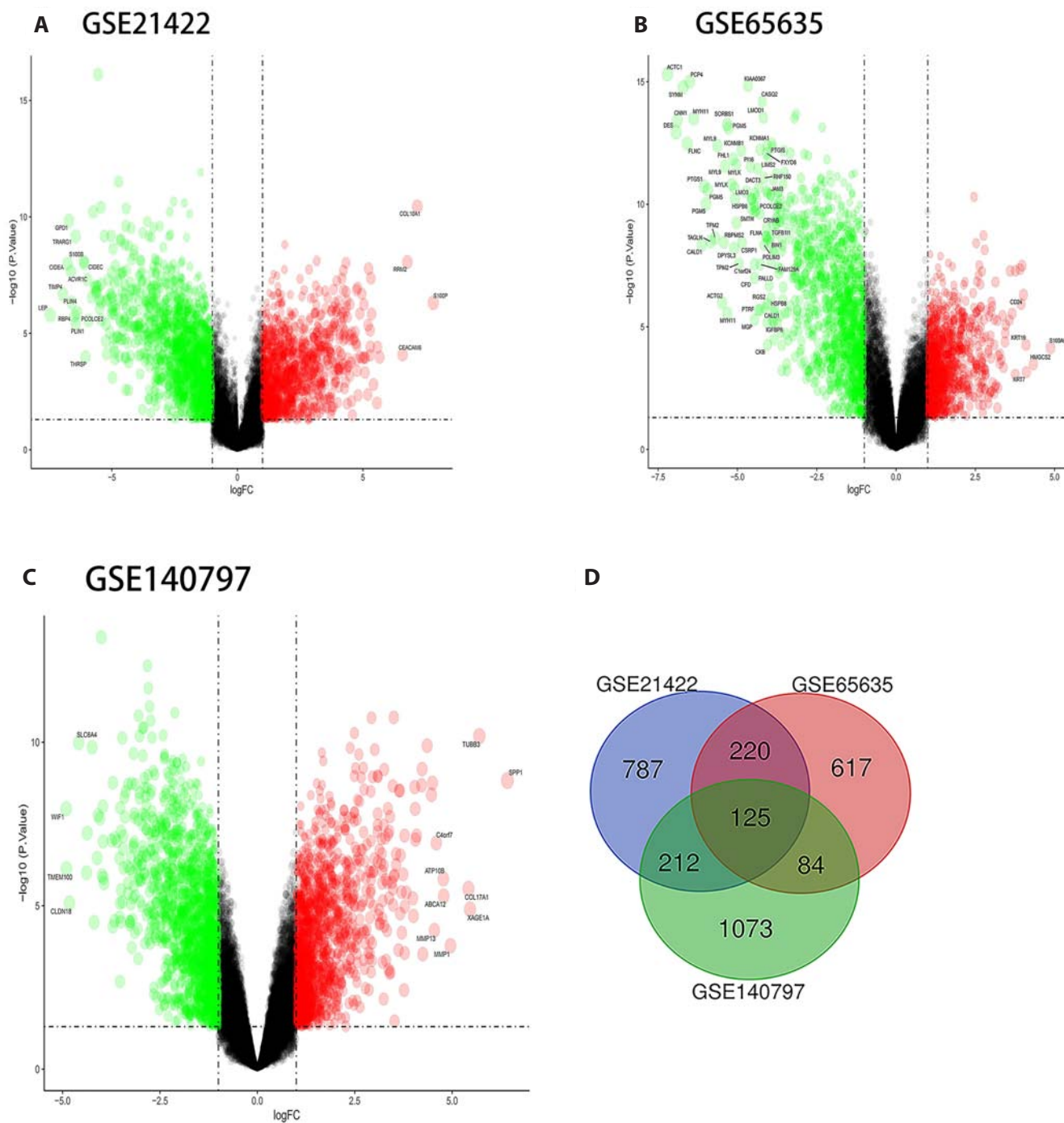
Fig. 1. Identification of expression differences between tumor and normal tissue. (A-C) Volcano plot of the differential mRNA expression analysis. X-axis: log2 fold change; Y-axis: –log10 (FDR p-value) for each probes; Vertical dotted lines: fold change > 1 or < –1; Horizontal dotted line: the significant cutoff (FDR p-value = 0.05). (A) There were 2,974 genes identified to be differentially expressed in GSE21422, including 1,344 up-regulated and 1,630 down-regulated genes. (B) 2,571 genes (1,195 up-regulated and 1,376 down-regulated genes) differentially expressed in GSE65635. (C) 3,442 genes (1,594 up-regulated and 1,848 down-regulated genes) differentially expressed in GSE140797. (D) A total of 125 genes were significantly differentially expressed in the three GEO datasets. (E, F) GO and KEGG pathway analysis of significant differetially expressed genes. (E) The top ten significantly enriched GO categories were calculated. Blue: Biological process; Orange: Cellular component; Green: Molecular function. (F) The cellular component was calculated. (G) Gene networks identified through KEGG analysis of the differentially expressed genes. GO, Gene Ontology; KEGG, Kyoto Encyclopedia of Genes and Genomes.

in cell division (Fig. 1E). For cellular components (CC), common DEGs were mainly involved in extracellular exosomes. For MF, common DEGs were mainly involved in the binding of identical proteins. Regarding KEGG pathways, common DEGs were abundant in cell cycle, oocyte meiosis, and progesterone-mediated oocyte matching (Fig. 1G). However, as this study focuses on CC,
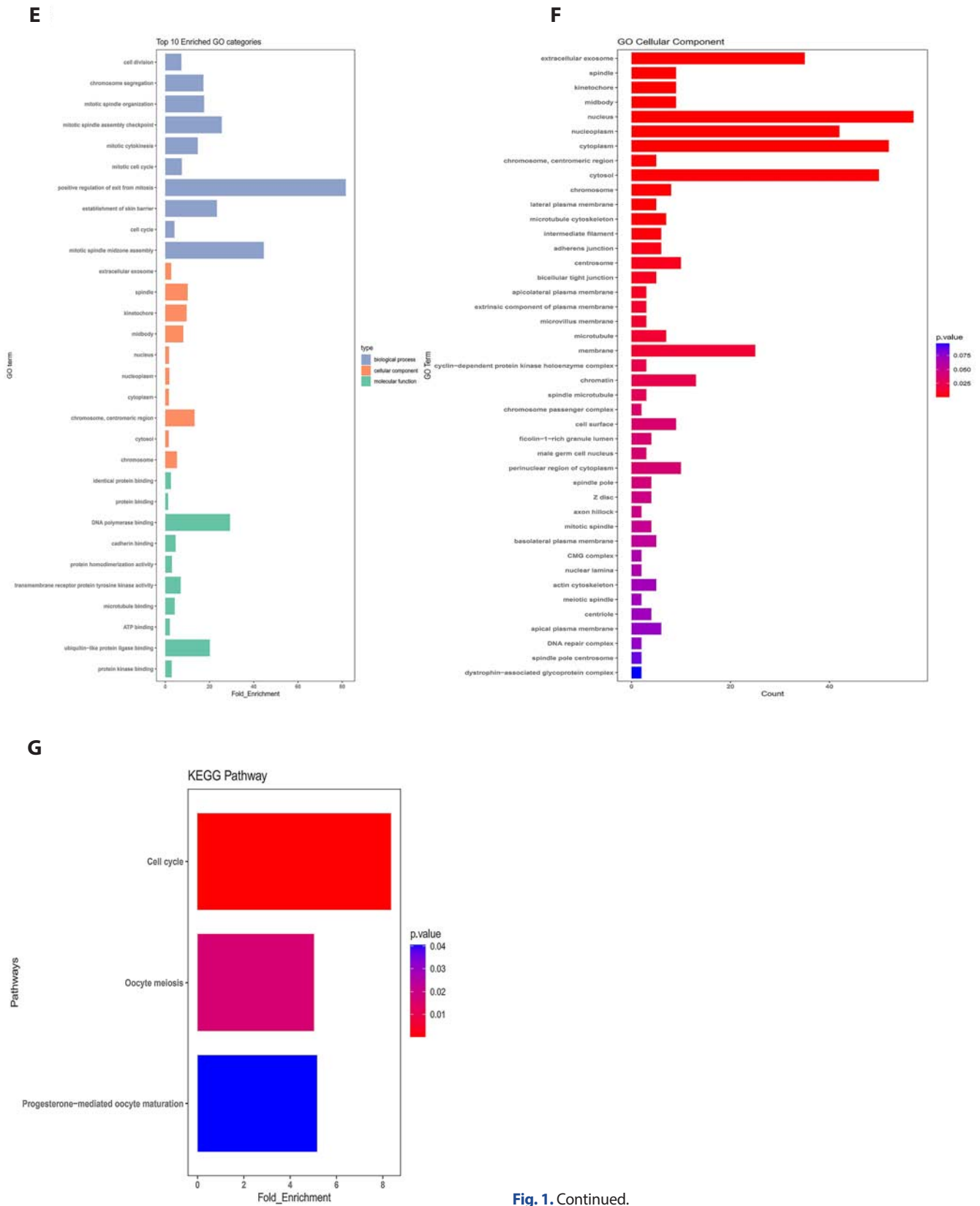
E

F

G

Fig. 1. Continued.

nine genes (CEACAM1, HM13, SDC1, CCR7, MST1R, HMMR, MIF, CD24, and PDIA4) enriched on the cell surface were identified as DRGs (Fig. 1F, Supplementary Table 1). The expression differences of these nine genes were analyzed (Fig. 2).
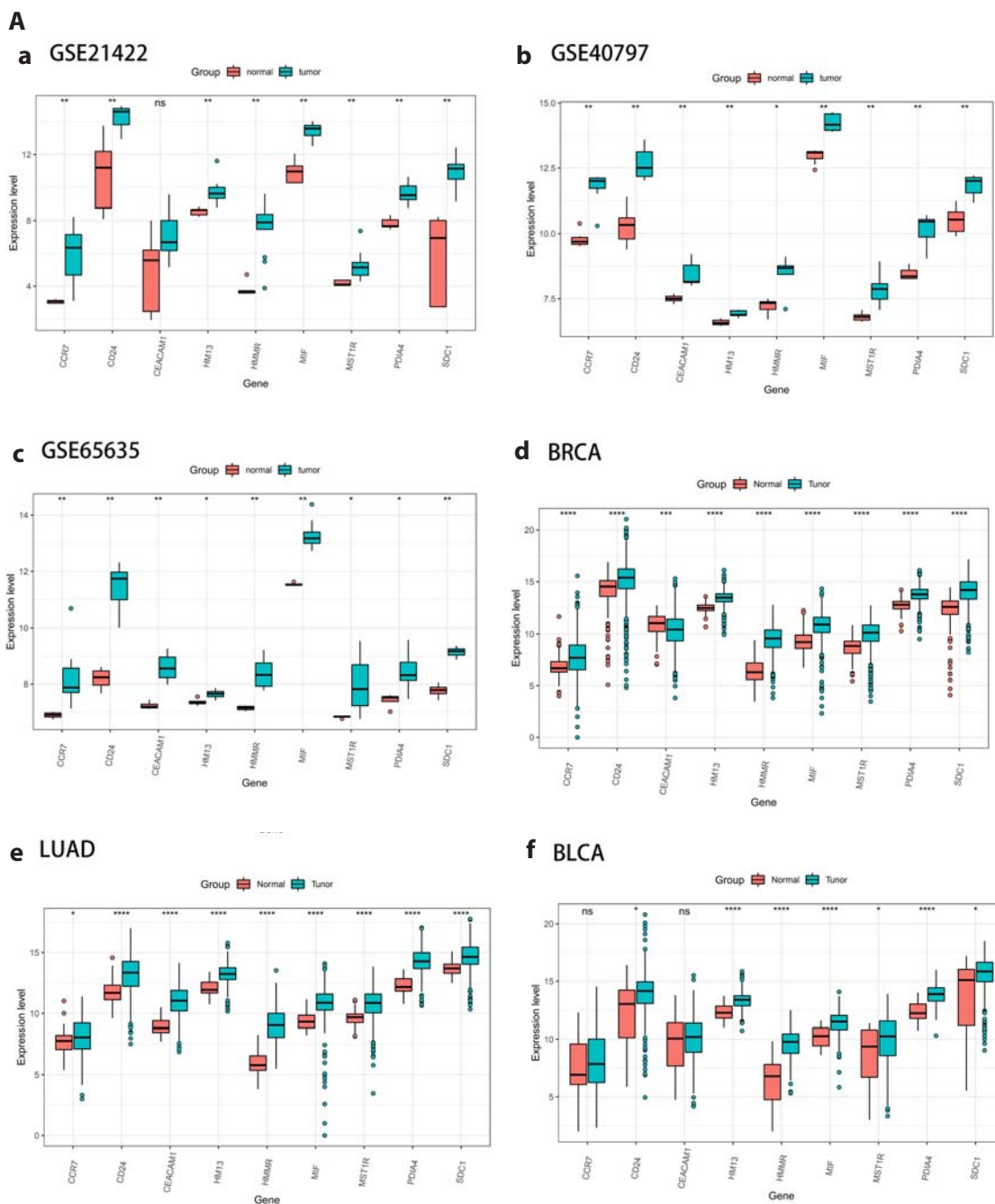
Fig. 2. Differential expression of common DEGs genes. (A) Differential expression of common DEGs genes in TCGA and GEO datasets. (B) Differential expression of common DEGs genes in TCGA according to clinical stage. (C) Survival analysis of MST1R in BRCA, LUAD, and BLCA datasets. *$p < 0.05$, **$p < 0.01$, ***$p < 0.005$, ****$p < 0.001$. DEGs, differentially expressed genes; ns, no significance.

## Differential expression of ordinary DEG genes was confirmed from the TCGA

BRCA, LUAD, and BLCA were selected from the TCGA, and gene expression differences were performed among common DEGs (Fig. 2Ad–f). According to analyses of gene expression differences, seven genes (HM13, SDC1, MST1R, HMMR, MIF, CD24, and PDIA4) were significantly different and were selected for further analysis.

Screening potential therapeutic target antigens of CAR-T cells

First, differential expression analysis of seven genes was carried out according to tumor stage (Fig. 2B). Except for the expression of MIF in LUAD and HM13 and of PDIA4 in BLCA, there were no significant differences of most genes at different stages. Second, we explored expressions of the seven genes in normal tissues using MERAV (Supplementary Fig. 1). CD24 was deleted because it was
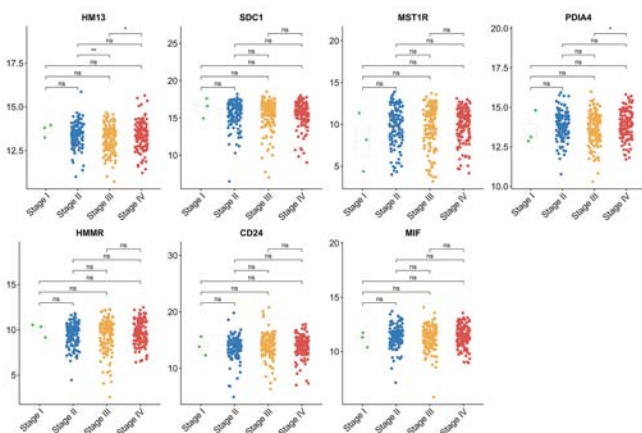
B

a BRCA
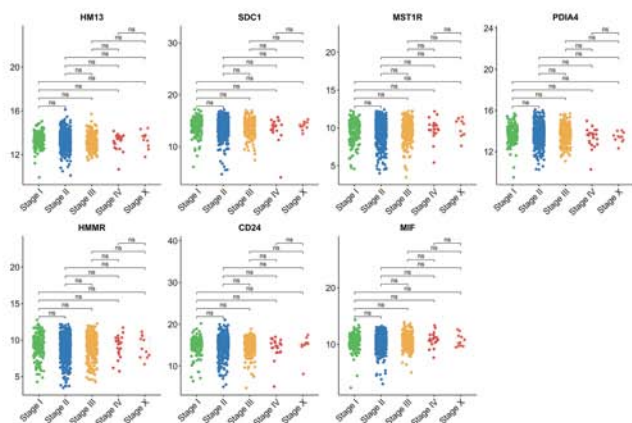
b LUAD
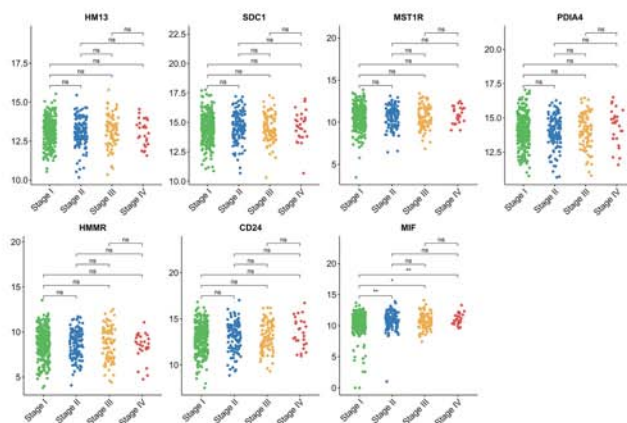
c BLCA

C

a

b

c

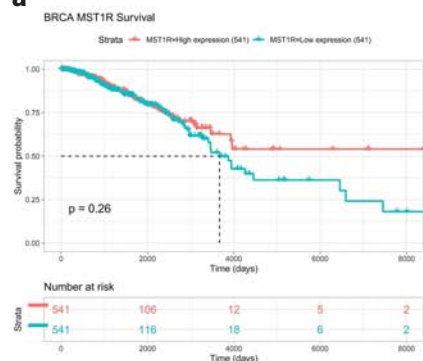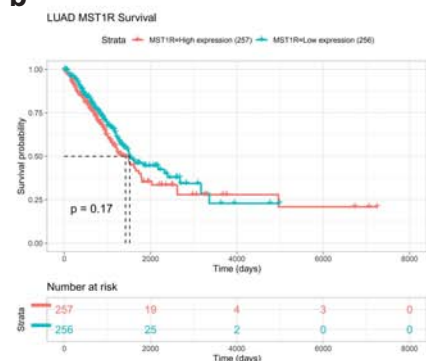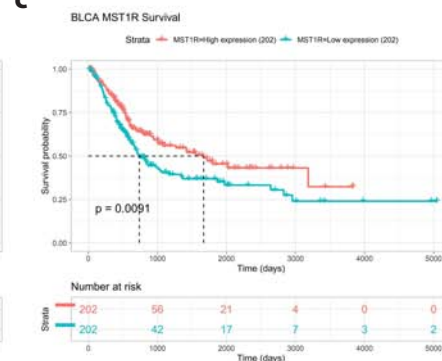**Fig. 2.** Continued.

not found in the MERAV. Combined with expression of the NCBI gene in the normal sequence of HPA RNA-seq, MST1R is a potential target antigen for CAR-T cell therapy for three kinds of tumors.

Survival analysis in three cancers showed that high expression of the MST1R gene influences the progression of bladder cancer and is a possible prognostic marker of bladder cancer (Fig. 2C).
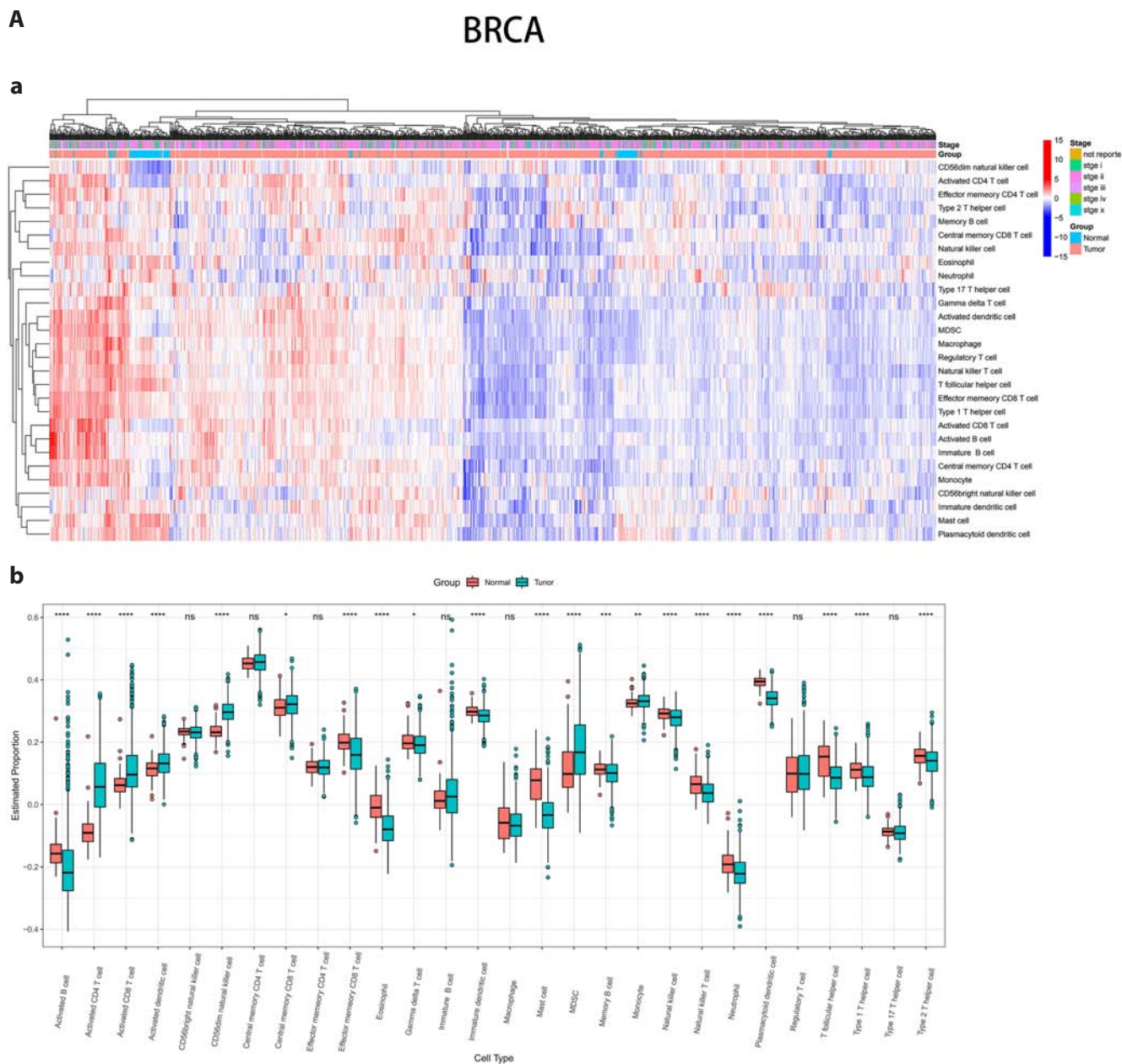
A

BRCA

a

b

Fig. 3. Correlation between immune infiltration and MST1R expression. A–C included (a) Heatmap of major immune cells, (b) boxplot of differential expression of 28 immune cells. *p < 0.05, **p < 0.01, ***p < 0.005, ****p < 0.001. ns, no significance.

Correlation between immune infiltration and MST1R expression

Many cell types driving immunosuppression can penetrate solid tumors in the tumor microenvironment, including myeloid-derived suppressor cells (MDSCs) and regulatory T cells (Tregs). These infiltrating and tumor cells promote the production of cytokines, chemokines, and growth factors, fostering tumor growth. In addition, immune checkpoints, such as PD-1 or CTLA-4, can reduce anti-tumor immunity. Therefore, it is necessary to analyze the tumor microenvironments of these three kinds of tumors. The infiltration levels of 28 kinds of immune cells and the scores

of chemokines and immune control points in each dataset were calculated by ssGESA analysis. Cox proportional hazards regression was used to evaluate the relationships between immune infiltration and patient survival rate of each cell type. Only significant results are shown in this manuscript.

The expression of MDSCs in normal BRCA tissues and tumor tissues is significantly different for immunosuppressed cells, and MDSCs and Tregs showed significant differences between LUAD and tumor tissues. However, there were no significant differences in BLCA. Univariate Cox regression analysis showed 5, 7, and 11 immune infiltrating cells in BRCA, LUAD and BLCA, respectively, which were significant for survival risk of breast cancer
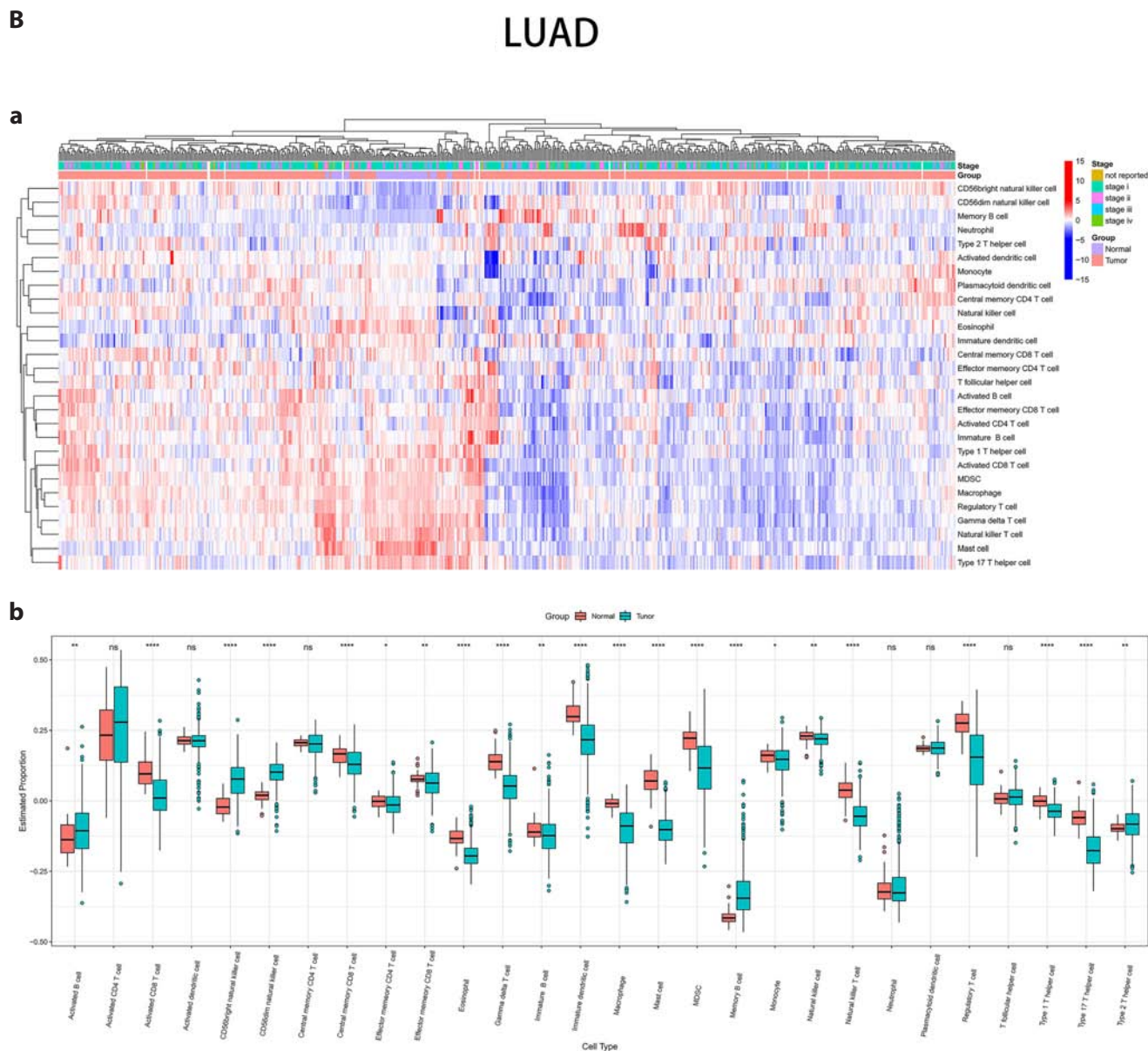
LUAD

B

a

b

Fig. 3. Continued.

(Supplementary Tables 2–4).

We found that the expression of MST1R in BRCA was significantly positively correlated with nine cell subsets (activated CD4 T cells, activated dendritic cells, CD56dim natural killer cells, central memory CD4 T cells, central memory CD8 T cells, immature B cells, immature dendritic cells, MDSCs, T_H17 (type 17 T helper) cell, but there were no significant differences in central memory CD4 T cells, central memory CD8 T cells, immature B cells, immature dendritic cells, MDSCs, or T_H17 cell, among which central memory CD8 T cells and natural killer cells were associated with poor prognosis (Fig. 3A, Supplementary Fig. 2A). The expression of MST1R in LUAD was significantly positively correlated with eight cell subsets (activated dendritic cells, CD-56dim natural killer cells, CD56bright natural killer cells, central

memory CD4 T cells, effector memory CD8 T cells, monocytes, neutrophils, T_H17 cell), but there were no significant differences in activated dendritic cells, CD56bright natural killer cells, effector memory CD8 T cells, monocytes, neutrophils, or T_H17 cell, among which T_H2 (type 2 T helper) cell, eosinophils, activated B cells, MDSCs, and activated dendritic cells were associated with poor prognosis (Fig. 3B, Supplementary Fig. 2B). The expression of MST1R in BLCA was significantly positively correlated with nine cell subsets (activated dendritic cells, CD56dim natural killer cells, central memory CD4 T cells, central memory CD8 T cells, immature dendritic cells, monocytes, natural killer cells, neutrophils, T_H17 cell), but there were no significant differences in activated dendritic cells, CD56dim natural killer cells, central memory CD4 T cells, central memory CD8 T cells, monocytes,
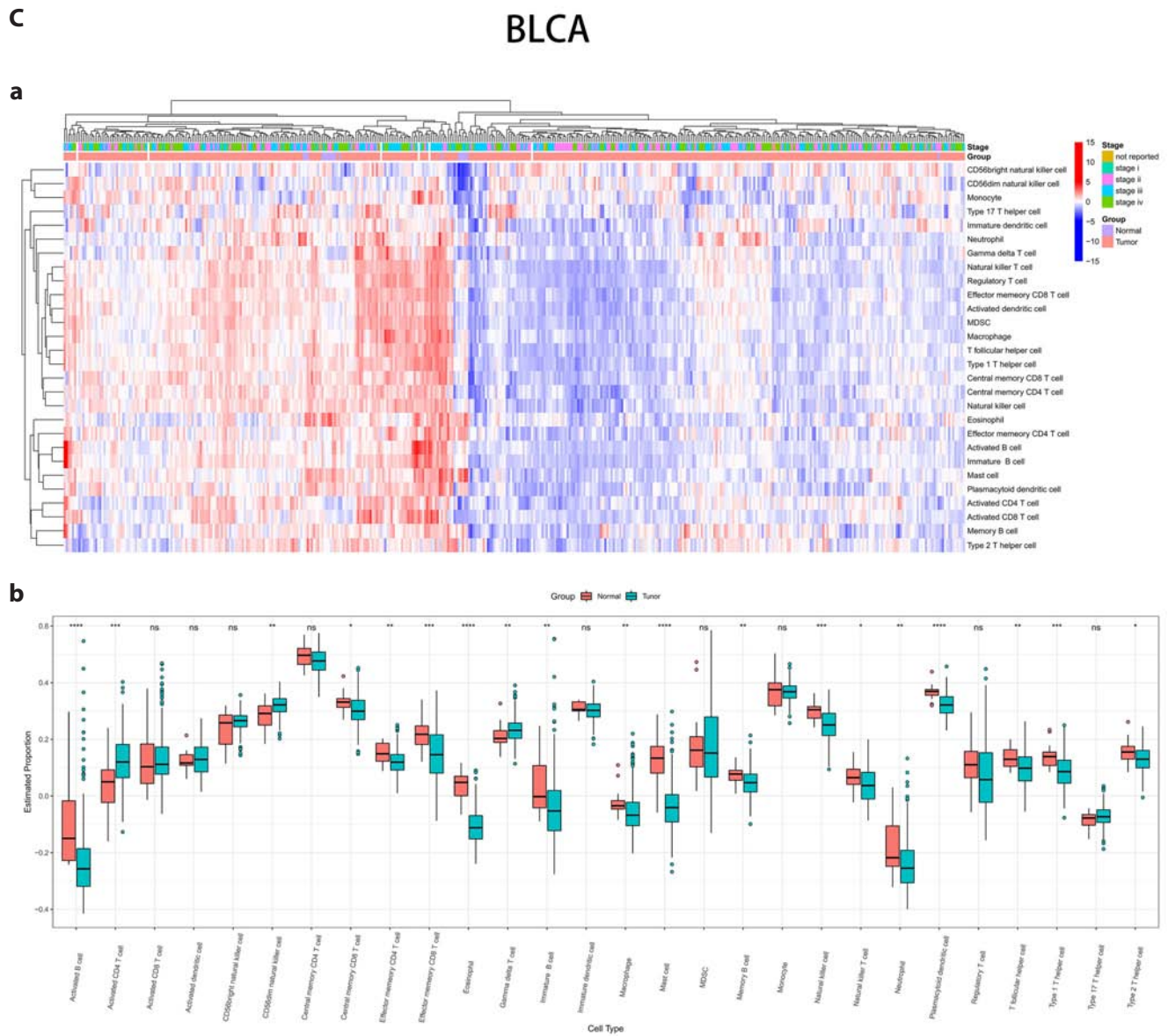
C

BLCA

a

b

Fig. 3. Continued.

natural killer cells, or neutrophils, among which activated CD8 T cells, mast cells, natural killer T cells, neutrophils, and CD-56bright natural killer cells were associated with poor prognosis (Fig. 3C, Supplementary Fig. 2C).

Correlations between chemokines and MST1R expression

Chemokines play important roles not only in the occurrence, promotion, and development of tumors, but also in regulating the infiltration of immune cells. To determine the chemokines related to immune cell infiltration, we evaluated the differential expression of 38 known chemokines between cancer tissues and normal tissues in breast cancer, lung adenocarcinoma and bladder cancer.

In addition to CCL15, CCL19, CCL22, CCL26, and CXCL8, 33

chemokines were found in BRCA and were expressed in tumor tissues. Univariate Cox regression analysis of 33 differentially expressed chemokines showed that CCL11, CCL17, CXCL9, CXCL13, CCCL1, CCL25, CXCL12, and CCL16 were significantly correlated with overall survival. In addition, systematic cluster correlation analysis was carried out to detect significant relationships between 10 variables (two cell subsets and eight chemokines). Finally, Spearman correlation analysis evaluated the relationships between the expression of MST1R and the eight chemokines. The results showed that CCL11, CCL17, CXCL9, CXCL13, CCL1, and CCL16 were positively correlated with MST1R, but CCL1 and CCL17 were not (Fig. 4A, Supplementary Fig. 3A). Except CCL27, CCL3, CCL5, CXCL1, CXCL11, XCL1, and XCL2, 31 chemokines were found in LUAD and were expressed in tumor tissues. Univariate Cox regression analysis of 33
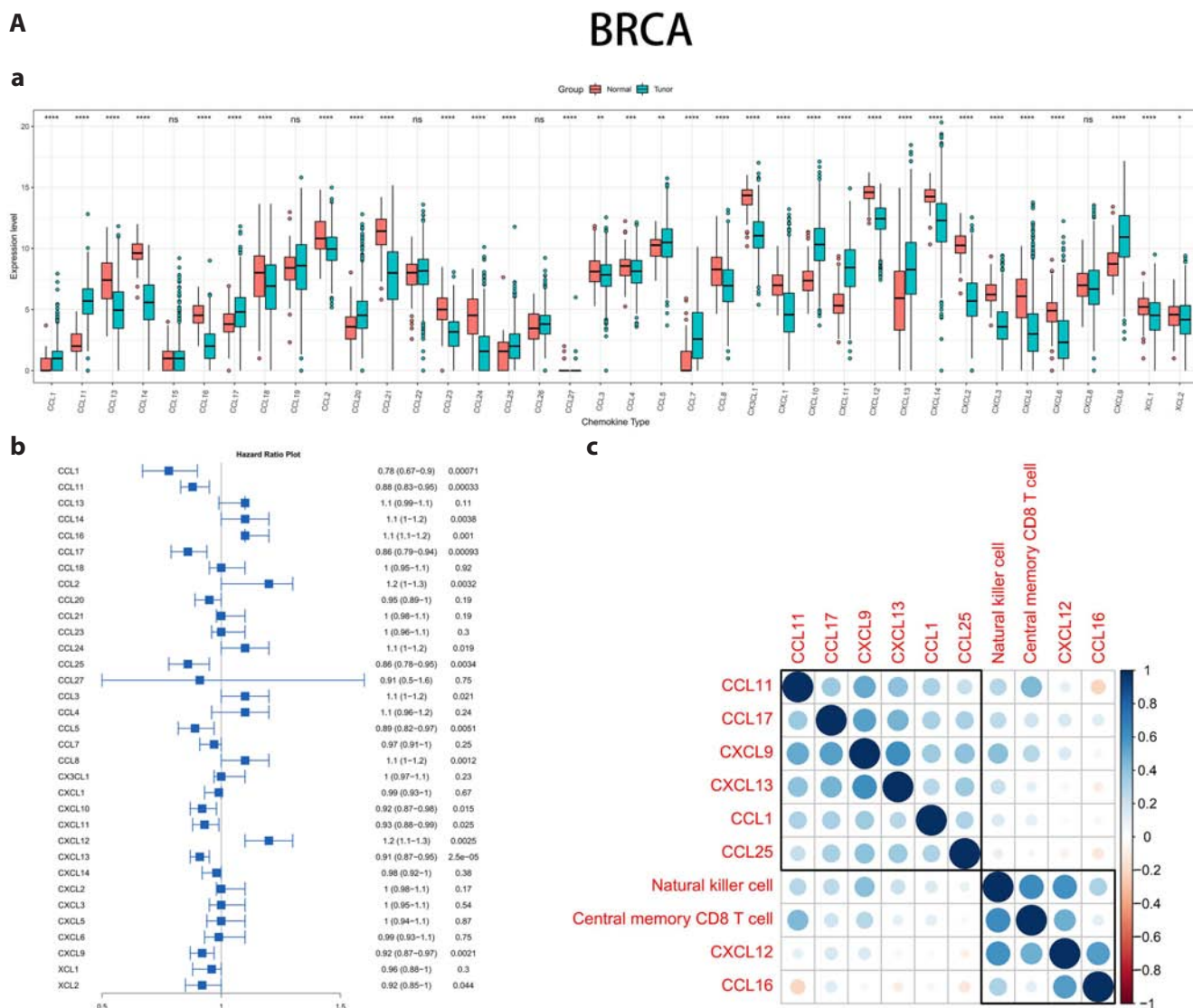
BRCA

A

a

b

c

Fig. 4. Correlation between chemokines and MST1R expression. A–C included (a) Differential expression of the 38 chemokines in normal and tumor tissues, (b) The univariate Cox regression analysis of differentially expressed chemokines. (c) Hierarchical clustering analysis was performed using Pearson's correlation coefficient. *p < 0.05, **p < 0.01, ***p < 0.005, ****p < 0.001. ns, no significance.

differentially expressed chemokines showed that CCL14, CCL16, CCL13, CCL17, and CX3CL1 were significantly correlated with overall survival. In addition, systematic cluster correlation analysis was carried out to identify significant relationships between 11 variables (six cell subsets and five chemokines). Finally, Spearman correlation analysis was used to evaluate the relationships between expression of MST1R and five chemokines. The results showed that CCL16, CCL13, CCL17, and CX3CL1 were positively correlated with MST1R (Fig. 4B, Supplementary Fig. 3B). In BLCA, we found that 18 chemokines (CCL13, CCL14, CCL16, CCL19, CCL2, CCL21, CCL23, CCL26, CCL4, CX3CL1, CXCL10, CXCL11, CXCL12, CXCL14, CXCL2, CXCL5, CXCL9, and XCL1) were significantly expressed in tumor tissues. Univariate Cox regression analysis of 31 chemokines with differential expression showed that CXCL11 and XCL1 were significantly correlated with

overall survival. In addition, systematic cluster correlation analysis was carried out to identify significant relationships between five cell subsets and two chemokines. Finally, Spearman correlation analysis was used to evaluate the relationships between expression of MST1R and that of two chemokines. CXCL11 was positively correlated with MST1R (Fig. 4C, Supplementary Fig. 3C).

Correlation between immune escape and MST1R expression

To determine the expression levels of immune escape-related factors in the tumor microenvironments of breast cancer, lung adenocarcinoma, and bladder cancer, we evaluated eight immune checkpoints (CD274 [PD-L1], CTLA4, HAVCR2, LAG3, PDCD1
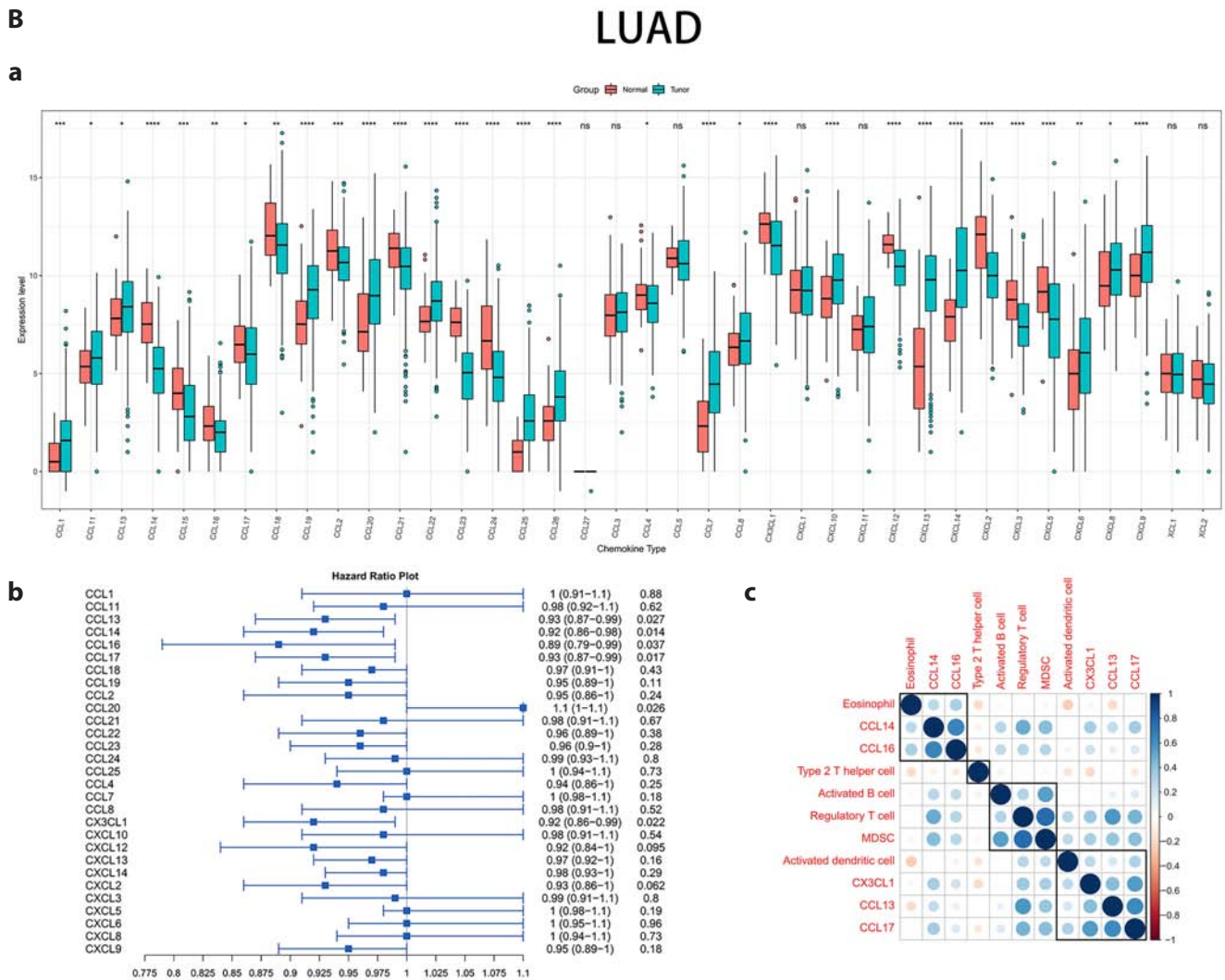
B

LUAD

a

b

c

Fig. 4. Continued.

[PD-1], PDCD1LG2 [PD-L2], TIGIT, and SIGLEC15), one cytokine (IFNG [IFN-γ]), and one growth factor (TGFB1 [TGF-β]). In BRCA, all genes were significantly overexpressed in cancer except PD-L1 and SIGLEC15. Other than PD-L2, all were positively correlated with MST1R expression (Fig. 5A, Supplementary Fig. 4A). In LUAD, all nine genes were highly expressed in cancer tissues except TGF-β. Ten genes were positively correlated with expression of MST1R, while PD-L 2 was not (Fig. 5B, Supplementary Fig. 4B). In BLCA, none of the 10 genes showed significantly high expression in cancer tissues. PD-L1, IFN-γ, 1 PD-1, SIGLEC15, and TGF-β were positively correlated with MST1R expression, but PD-L1, IFN-γ and PD-1 were not (Fig. 5C, Supplementary Fig. 4C).

DISCUSSION

CAR is the core component of CAR-T, which endows T cells

with the ability to recognize tumor antigens in a non-human leukocyte antigen manner instead of using natural T cell surface antibodies. CAR includes a TAA binding domain (usually scFv fragments from the antigen binding domain of monoclonal antibodies), an extracellular hinge domain, a transmembrane domain, and an intracellular signal domain [11,12]. We used bioinformatics to predict MST1R as a potential new target antigen of CAR-T cell therapy for breast cancer, lung adenocarcinoma, and bladder cancer. However, there are some obstacles in treating solid tumors with CAR-T cells.
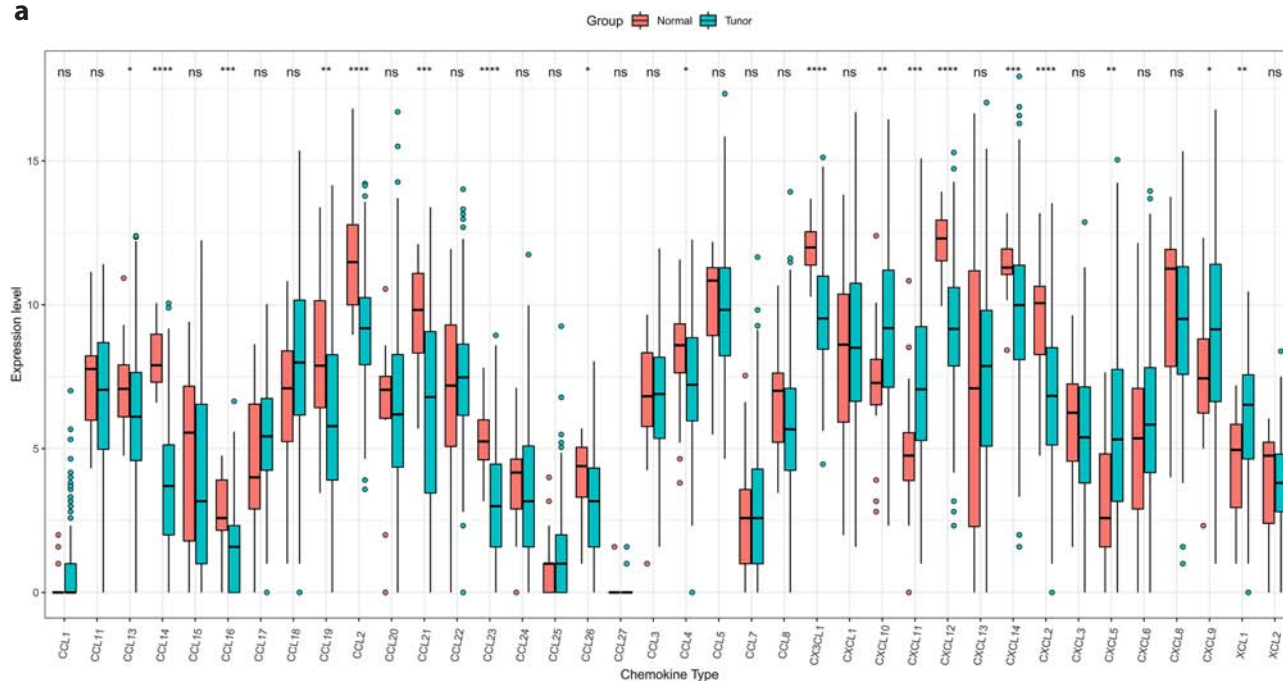
Immunosuppression of solid tumor microenvironment

As outlined above, MDSCs and Tregs play roles in protecting solid tumor cells from being killed by the host immune system in the tumor microenvironment. Some chemokines, such as CXCL1, CXCL12, and CXCL5, are secreted by solid tumors and prevent T
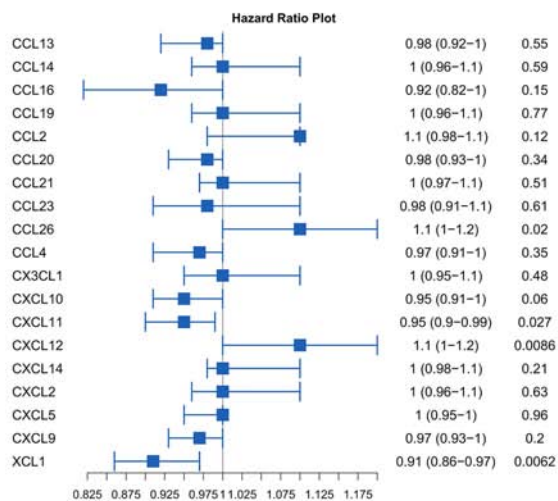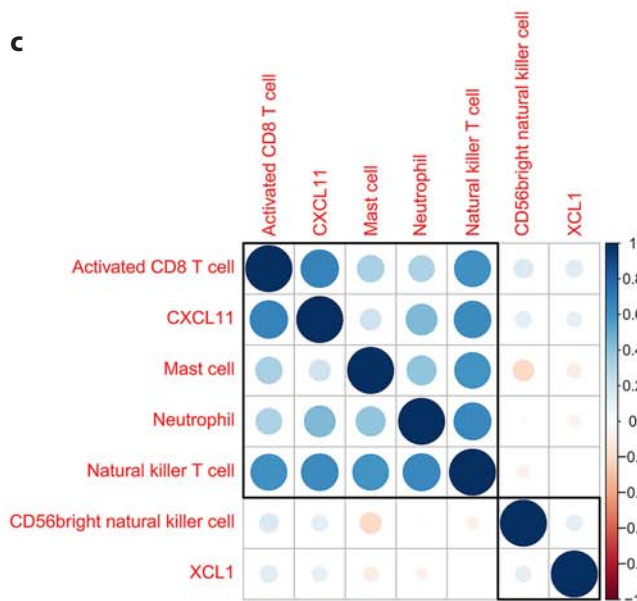
C

BLCA

a

b

c

Fig. 4. Continued.

cells from migrating and infiltrating into tumor lesions [13-15]. Multiple chemokine/chemokine receptor pairs, including CCL2/CCR2, CCL5/CCR5/, CXCL5/CXCR2, and CXCL12/CXCR4, have been reported to indirectly promote tumor progression by increasing the recruitment and suppressive activity of MDSCs [16]. Tumor-derived cytokines are soluble factors that hinder the effect of tumor immunotherapy on solid tumors. TGF-β is a constant tumor cytokine that plays a major role in alleviating anti-tumor

response [17]. In CAR-T therapy for solid tumors, PD-L1 inhibits CAR-T cell activation by binding to PD-1. In addition, immune checkpoints such as PD-1 or CTLA-4 can reduce anti-tumor immunity [18,19]. Studies have shown that the effective anti-tumor activity of CAR-T cells depends on IFN-γ signals, including IFN-γ secreted by CAR-T and IFN-γ signals in immune cells [20].

The results of this study showed that, in breast cancer, MDSCs, CXCL1, CXCL12, CXCL5, CCL2, CCL5, TGF-β, CTLA-4, and
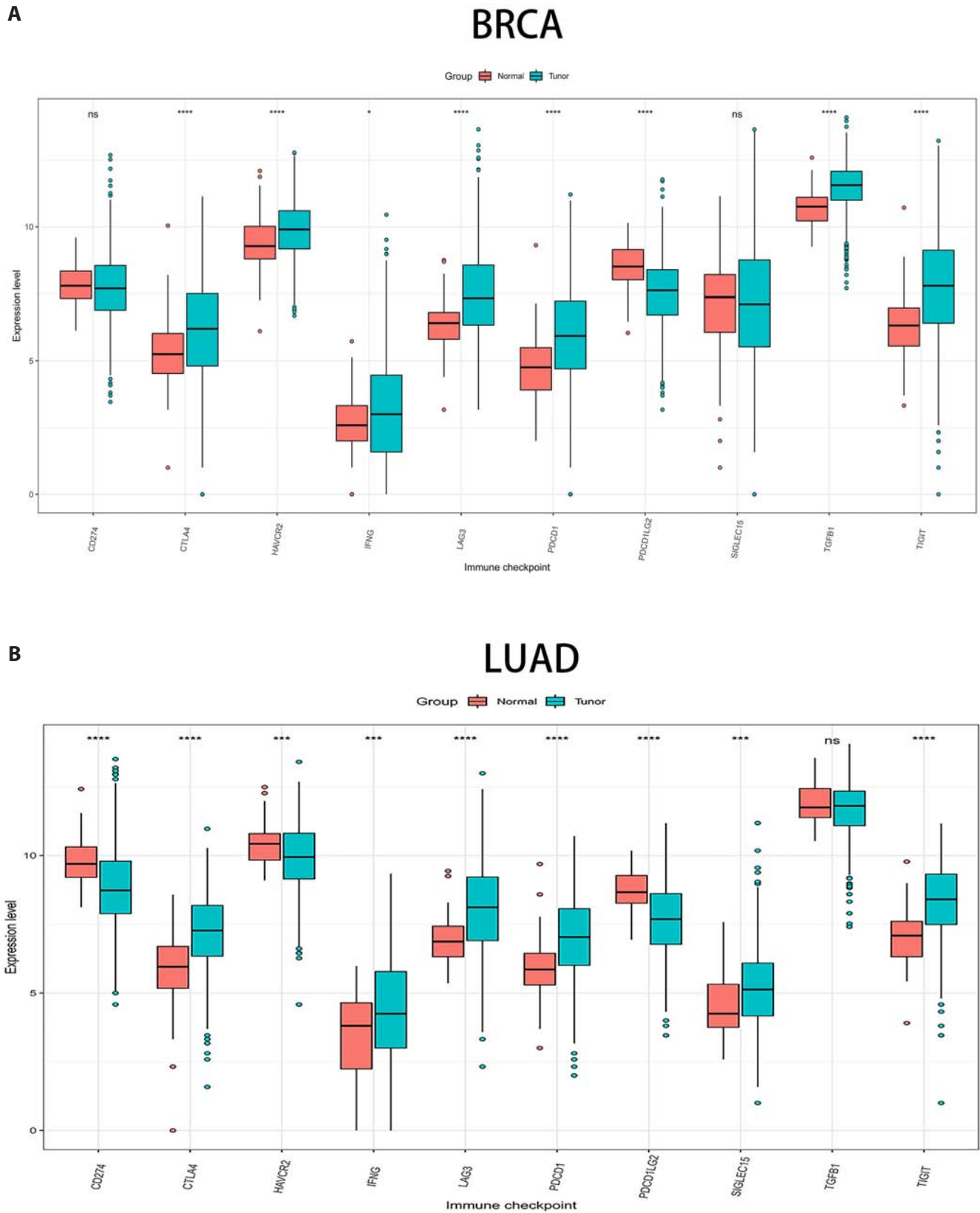
A

B

Fig. 5. Correlation between immune checkpoint genes and MST1R expression. A–C included differential expression of the 10 immune checkpoint genes in normal and tumor tissues. *p < 0.05, **p < 0.01, ***p < 0.005, ****p < 0.001. ns, no significance.
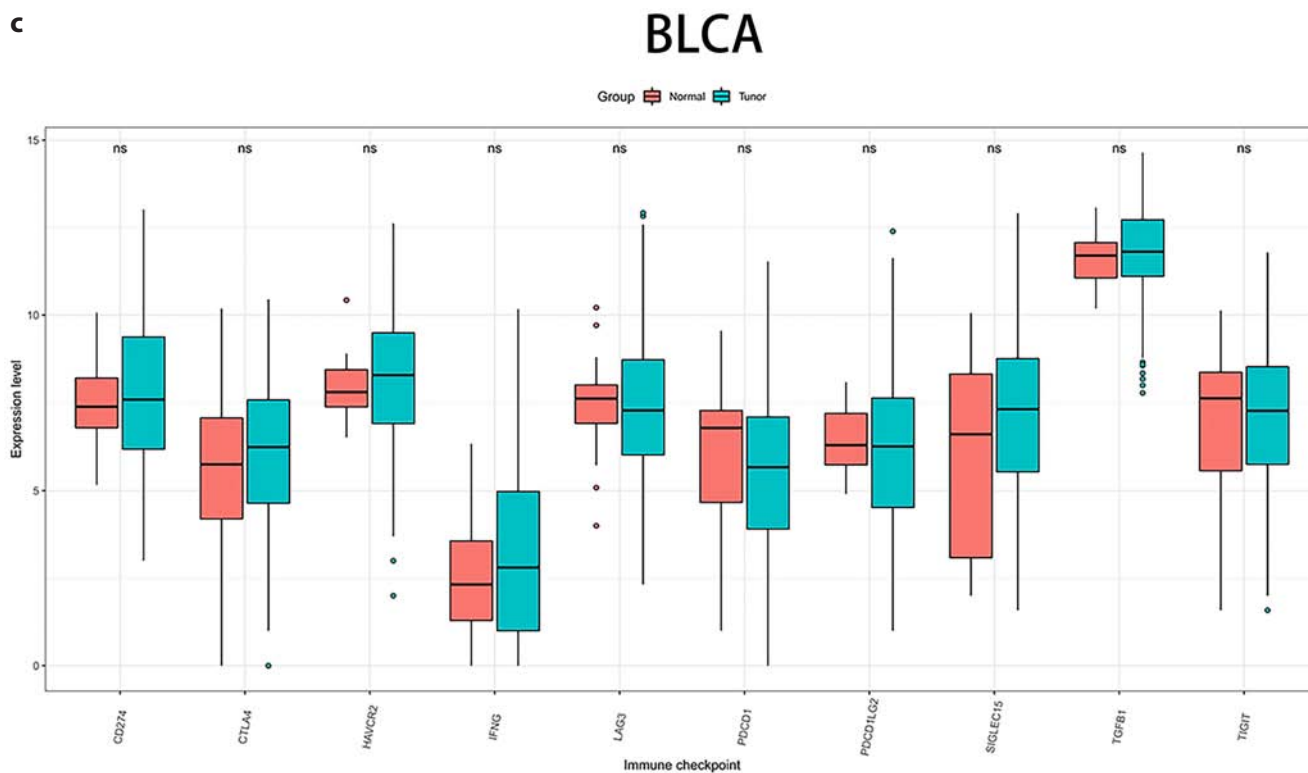
C

Fig. 5. Continued.

IFN-γ were significantly overexpressed in tumor tissues, while PD-L1 was not. MST1R expression was positively correlated with TGF-β, CTLA-4, and IFN-γ. In lung adenocarcinoma, MDSCs, Tregs, CXCL12, CXCL5, CCL2, PD-L1, CTLA-4, and IFN-γ were significantly overexpressed in tumor tissues, but TGF-β was not. MST1R expression was positively correlated with TGF-β, CTLA-4, and IFN-γ. However, in bladder cancer, CXCL12, CCL2, and CXCL5 were significantly overexpressed in tumor tissues, while MDSCs, Tregs, PD-L1, TGF-β, CTLA-4, and IFN-γ were not. MST1R expression was positively correlated with TGF-β. Moreover, high expression of the MST1R gene has influence on the progression of bladder cancer and can be used as a progression indicator of bladder cancer.

Clinicians and researchers should pay attention to the existence of immune suppression in tumor microenvironments when developing CAR-T cell therapy for breast cancer, lung adenocarcinoma, and bladder cancer. Persistence and function of T cells can be ensured by combining immunotherapy with checkpoint blocking agents. A study of 14 children with recurrent B-ALL conducted at Children's Hospital of Philadelphia, Pennsylvania, showed that the combination of PD-1 blockade pretreatment with CD19 CAR-T cells improved the durability and therapeutic effect of CAR-T cells [21]. Due to the lack of chemokine receptor expression on T cells, it is difficult for CAR-T cells to transport and infiltrate into tumor sites, which greatly hinders their ability to kill tumors. T cells can be reoriented to tumor sites by modifying them to express chemokine receptors that match the correspond-

ing tumor-derived chemokines. Previous studies have shown that T cells engineered with chemokine receptor (CXCL1 receptor) can drive their own migration to melanoma cells [13]. The function of CD8+ T cells can also be improved by neutralizing TGF-β with antibodies or small molecule drugs. Pre-clinical data show that integration of costimulatory molecules into CAR is helpful for CAR-T cells to reverse the immune suppressed tumor microenvironment. For example, CD28 co-stimulation overcomes TGF-β-mediated proliferation inhibition of proliferation of redirected human CD4+ and CD8+ cells in an antitumor cell attack[22] and enhances the resistance of T cells to Treg cells [22,23].

Strategies to improve CAR

Because MST1R does not have antigen specificity, methods are needed to impart this feature. First, due to the low expression of MST1R in normal tissues, the affinity of scFv has been adjusted to ignore normal tissues with low expression. Hudecek *et al.* [24] reported that different scFv with the same CAR configuration demonstrate variable receptor affinity, as do different hinge domains of the same scFv [24,25]. Therefore, choosing an appropriate configuration is a crucial part of CAR design. Second, CAR configurations can be improved, into such structures as two (bispecific [bi]CARs) [26] SynNotch receptors [27,28] that are controlled by logic gates, and recognize ligands on a cell surface to trigger inducible target gene expression. These configurations are designed to recognize TAA and induce the expression of CAR

and can trigger T cells to activate a second TAA and other new CAR configurations and to recognize antigen specificity. "Off switches," or suicide genes, can be added to minimize adverse events and maximize the safety of CAR-T designs to reduce unwanted toxicity. Suicide genes include HSV-TK, CD20, inducible caspase 9 (iCas 9), and truncated EGFR (tEGFR or EGFRt) [29-32].

Macrophages stimulate RTK receptor 1 or MST1R, also known as RON (récepteur d'origin Nantais), which encodes a 180 kDa receptor [33]. RON activation contributes to tumor progression and metastasis by promoting cell proliferation and motility and inhibiting apoptosis [33,34]. Some studies have shown that RON is expressed not only in tumor microenvironments (tumor-associated macrophages and MDSC), but also in solid tumors (breast cancer, lung cancer, bladder cancer) [34].

Based on bioinformatics analysis and previous reports, combined with modifications of CAR configurations and necessary treatments, MST1R may become a new target antigen for the treatment of three kinds of cancers. However, there are some limitations of this study. We conducted only theoretical analysis, and the corresponding experimental verification was not carried out by designing a CAR.

We used bioinformatics analysis to determine that MST1R is a feasible potential target antigen for therapy of three kinds of solid tumor. In addition, MST1R can be used as an indicator of progression of bladder cancer.

FUNDING

ACKNOWLEDGEMENTS

CONFLICTS OF INTEREST

The authors declare no conflicts of interest.

SUPPLEMENTARY MATERIALS

Supplementary data including four tables and four figures can be found with this article online at https://doi.org/10.4196/kjpp.2023.27.3.241.

REFERENCES

1. Abramson JS. Anti-CD19 CAR T-cell therapy for B-cell Non-Hodg-

kin lymphoma. *Transfus Med Rev.* 2020;34:29-33.
2. Feng D, Sun J. Overview of anti-BCMA CAR-T immunotherapy for multiple myeloma and relapsed/refractory multiple myeloma. *Scand J Immunol.* 2020;92:e12910.
3. Martinez M, Moon EK. CAR T cells for solid tumors: new strategies for finding, infiltrating, and surviving in the tumor microenvironment. *Front Immunol.* 2019;10:128.
4. Kloss CC, Condomines M, Cartellieri M, Bachmann M, Sadelain M. Combinatorial antigen recognition with balanced signaling promotes selective tumor eradication by engineered T cells. *Nat Biotechnol.* 2013;31:71-75.
5. Xie Y, Hu Y, Zhou N, Yao C, Wu L, Liu L, Chen F. CAR T-cell therapy for triple-negative breast cancer: where we are. *Cancer Lett.* 2020;491:121-131.
6. Ritchie ME, Phipson B, Wu D, Hu Y, Law CW, Shi W, Smyth GK. limma powers differential expression analyses for RNA-sequencing and microarray studies. *Nucleic Acids Res.* 2015;43:e47.
7. Huang da W, Sherman BT, Lempicki RA. Bioinformatics enrichment tools: paths toward the comprehensive functional analysis of large gene lists. *Nucleic Acids Res.* 2009;37:1-13.
8. Liu R, Guo CX, Zhou HH. Network-based approach to identify prognostic biomarkers for estrogen receptor-positive breast cancer treatment with tamoxifen. *Cancer Biol Ther.* 2015;16:317-324.
9. Shaul YD, Yuan B, Thiru P, Nutter-Upham A, McCallum S, Lanzkron C, Bell GW, Sabatini DM. MERAV: a tool for comparing gene expression across human tissues and cell types. *Nucleic Acids Res.* 2016;44:D560-D566.
10. Bindea G, Mlecnik B, Tosolini M, Kirilovsky A, Waldner M, Obenauf AC, Angell H, Fredriksen T, Lafontaine L, Berger A, Bruneval P, Fridman WH, Becker C, Pagès F, Speicher MR, Trajanoski Z, Galon J. Spatiotemporal dynamics of intratumoral immune cells reveal the immune landscape in human cancer. *Immunity.* 2013;39:782-795.
11. Sadelain M, Rivière I, Brentjens R. Targeting tumours with genetically enhanced T lymphocytes. *Nat Rev Cancer.* 2003;3:35-45.
12. Bridgeman JS, Hawkins RE, Hombach AA, Abken H, Gilham DE. Building better chimeric antigen receptors for adoptive T cell therapy. *Curr Gene Ther.* 2010;10:77-90.
13. Kershaw MH, Wang G, Westwood JA, Pachynski RK, Tiffany HL, Marincola FM, Wang E, Young HA, Murphy PM, Hwu P. Redirecting migration of T cells to chemokine secreted from tumors by genetic modification with CXCR2. *Hum Gene Ther.* 2002;13:1971-1980.
14. Wang G, Lu X, Dey P, Deng P, Wu CC, Jiang S, Fang Z, Zhao K, Konaparthi R, Hua S, Zhang J, Li-Ning-Tapia EM, Kapoor A, Wu CJ, Patel NB, Guo Z, Ramamoorthy V, Tieu TN, Heffernan T, Zhao D, *et al.* Targeting YAP-dependent MDSC infiltration impairs tumor progression. *Cancer Discov.* 2016;6:80-95.
15. Feig C, Jones JO, Kraman M, Wells RJ, Deonarine A, Chan DS, Connell CM, Roberts EW, Zhao Q, Caballero OL, Teichmann SA, Janowitz T, Jodrell DI, Tuveson DA, Fearon DT. Targeting CXCL12 from FAP-expressing carcinoma-associated fibroblasts synergizes with anti-PD-L1 immunotherapy in pancreatic cancer. *Proc Natl Acad Sci U S A.* 2013;110:20212-20217.
16. Marcuzzi E, Angioni R, Molon B, Calì B. Chemokines and chemokine receptors: orchestrating tumor metastasization. *Int J Mol Sci.* 2018;20:96. Erratum in: *Int J Mol Sci.* 2019;20:2651.
17. Xia AL, Wang XC, Lu YJ, Lu XJ, Sun B. Chimeric-antigen receptor

T (CAR-T) cell therapy for solid tumors: challenges and opportunities. *Oncotarget.* 2017;8:90521-90531.

18. Sterner RC, Sterner RM. CAR-T cell therapy: current limitations and potential strategies. *Blood Cancer J.* 2021;11:69.

19. Ma S, Li X, Wang X, Cheng L, Li Z, Zhang C, Ye Z, Qian Q. Current progress in CAR-T cell therapy for solid tumors. *Int J Biol Sci.* 2019;15:2548-2560.

20. Alizadeh D, Wong RA, Gholamin S, Maker M, Aftabizadeh M, Yang X, Pecoraro JR, Jeppson JD, Wang D, Aguilar B, Starr R, Larmonier CB, Larmonier N, Chen MH, Wu X, Ribas A, Badie B, Forman SJ, Brown CE. IFNγ is critical for CAR T cell-mediated myeloid activation and induction of endogenous immunity. *Cancer Discov.* 2021;11:2248-2265.

21. Li AM, Hucks GE, Dinofia AM, Seif AE, Teachey DT, Baniewicz D, Callahan C, Fasano C, McBride B, Gonzalez V, Nazimuddin F, Porter DL, Lacey SF, June CH, Grupp SA, Maude SL. Checkpoint inhibitors augment CD19-directed chimeric antigen receptor (CAR) T cell therapy in relapsed B-cell acute lymphoblastic leukemia. *Blood.* 2018;132(Suppl 1):556.

22. Koehler H, Kofler D, Hombach A, Abken H. CD28 costimulation overcomes transforming growth factor-beta-mediated repression of proliferation of redirected human CD4$^+$ and CD8$^+$ T cells in an antitumor cell attack. *Cancer Res.* 2007;67:2265-2273.

23. Loskog A, Giandomenico V, Rossig C, Pule M, Dotti G, Brenner MK. Addition of the CD28 signaling domain to chimeric T-cell receptors enhances chimeric T-cell resistance to T regulatory cells. *Leukemia.* 2006;20:1819-1828.

24. Hudecek M, Lupo-Stanghellini MT, Kosasih PL, Sommermeyer D, Jensen MC, Rader C, Riddell SR. Receptor affinity and extracellular domain modifications affect tumor recognition by ROR1-specific chimeric antigen receptor T cells. *Clin Cancer Res.* 2013;19:3153-3164.

25. Duan Y, Chen R, Huang Y, Meng X, Chen J, Liao C, Tang Y, Zhou C, Gao X, Sun J. Tuning the ignition of CAR: optimizing the affinity of scFv to improve CAR-T therapy. *Cell Mol Life Sci.* 2021;79:14.

26. Feng Y, Liu X, Li X, Zhou Y, Song Z, Zhang J, Shi B, Wang J. Novel BCMA-OR-CD38 tandem-dual chimeric antigen recep-

tor T cells robustly control multiple myeloma. *Oncoimmunology.* 2021;10:1959102.

27. Roybal KT, Rupp LJ, Morsut L, Walker WJ, McNally KA, Park JS, Lim WA. Precision tumor recognition by T cells with combinatorial antigen-sensing circuits. *Cell.* 2016;164:770-779.

28. Choe JH, Watchmaker PB, Simic MS, Gilbert RD, Li AW, Krasnow NA, Downey KM, Yu W, Carrera DA, Celli A, Cho J, Briones JD, Duecker JM, Goretsky YE, Dannenfelser R, Cardarelli L, Troyanskaya O, Sidhu SS, Roybal KT, Okada H, *et al.* SynNotch-CAR T cells overcome challenges of specificity, heterogeneity, and persistence in treating glioblastoma. *Sci Transl Med.* 2021;13:eabe7378.

29. Di Stasi A, Tey SK, Dotti G, Fujita Y, Kennedy-Nasser A, Martinez C, Straathof K, Liu E, Durett AG, Grilley B, Liu H, Cruz CR, Savoldo B, Gee AP, Schindler J, Krance RA, Heslop HE, Spencer DM, Rooney CM, Brenner MK. Inducible apoptosis as a safety switch for adoptive cell therapy. *N Engl J Med.* 2011;365:1673-1683.

30. Ciceri F, Bonini C, Stanghellini MT, Bondanza A, Traversari C, Salomoni M, Turchetto L, Colombi S, Bernardi M, Peccatori J, Pescarollo A, Servida P, Magnani Z, Perna SK, Valtolina V, Crippa F, Callegaro L, Spoldi E, Crocchiolo R, Fleischhauer K, *et al.* Infusion of suicide-gene-engineered donor lymphocytes after family haploidentical haemopoietic stem-cell transplantation for leukaemia (the TK007 trial): a non-randomised phase I-II study. *Lancet Oncol.* 2009;10:489-500.

31. Marin V, Cribioli E, Philip B, Tettamanti S, Pizzitola I, Biondi A, Biagi E, Pule M. Comparison of different suicide-gene strategies for the safety improvement of genetically manipulated T cells. *Hum Gene Ther Methods.* 2012;23:376-386.

32. Jones BS, Lamb LS, Goldman F, Di Stasi A. Improving the safety of cell therapy products by suicide gene transfer. *Front Pharmacol.* 2014;5:254.

33. Robert C, Marquevielle J, Salgado GF. The promoter region of the proto-oncogene MST1R contains the main features of G-quadruplexes formation. *Int J Mol Sci.* 2022;23:12905.

34. Cazes A, Childers BG, Esparza E, Lowy AM. The MST1R/RON tyrosine kinase in cancer: oncogenic functions and therapeutic strategies. *Cancers (Basel).* 2022;14:2037.